ELSEVIER

Journal of Computational and Applied Mathematics 96 (1998) 99–116

JOURNAL OF
COMPUTATIONAL AND
APPLIED MATHEMATICS

A posteriori L^2-error estimates for the nonconforming P_1/P_0-finite element discretization of the Stokes equations

Volker John*

Otto-von-Guericke-Universität Magdeburg, Institut für Analysis und Numerik, Postfach 4120, D-39016 Magdeburg, Germany

Received 3 December 1997; received in revised form 30 April 1998

Abstract

This paper focusses on a residual-based a posteriori error estimator for the L^2-error of the velocity for the nonconforming P_1/P_0-finite element discretization of the Stokes equations. We derive an a posteriori error estimator which yields a local lower as well as a global upper bound on the error. Numerical tests demonstrate the efficiency of the global error estimator and give a comparison with respect to the adaptive grid refinement to an a posteriori error estimator in the discrete energy norm proposed by Dari et al. (1995). © 1998 Elsevier Science B.V. All rights reserved.

AMS classification: 65N15, 65N30, 65N50

Keywords: Stokes equations; Nonconforming finite element methods; Residual-based a posteriori error estimators; Adaptive grid refinement

1. Introduction

The use of a posteriori error estimators for estimating the global error as well as for obtaining information for adaptive techniques is nowadays a standard component of numerical codes for solving partial differential equations.

Rigorous analysis of a posteriori error estimators started at the end of the 1970s by the pioneering paper of Babuška and Rheinboldt [2]. During the 1980s and at the beginning of the 1990s, fundamental and general approaches for analyzing a posteriori error estimators for conforming finite element solutions of many classes of partial differential equations have been developed, e.g. in [1, 10, 16]. In these papers, the conformity of the finite element space, or more generally the orthogonality of the Galerkin approach for conforming finite element methods plays an essential rôle. However,

* E-mail: volker.john@mathematik.uni-magdeburg.de.

0377-0427/98/$19.00 © 1998 Elsevier Science B.V. All rights reserved
PII S0377-0427(98)00095-8

discretizations which are violating this Galerkin orthogonality are of substantial importance in applications, such as the use of numerical integration, upwind stabilization techniques for convection dominated problems or nonconforming finite element discretizations in computational fluid dynamics (CFD). Nonconforming finite element discretizations in CFD easily fulfill the Babuška–Brezzi stability condition [6, 13] and have advantages on parallel computers [9, 14].

A posteriori error estimators for nonconforming discretizations have been investigated only in a couple of papers. Residual-based a posteriori error estimators for the nonconforming P_1-discretization of the Laplace equation and the error in the element-wise computed H^1-norm have been developed in [8, 19]. In comparison to related error estimators for conforming finite element discretizations, an additional term which measures the nonconformity of the discrete solution occurs. The approach in [8] has been extended to the Stokes equations and the error in the discrete energy norm in [7].

The plan of the paper is the following. In Section 2, the equations and notations are introduced and mathematical preliminaries are given. The construction of the special cutoff function B_E in Section 3 enables us to prove a local lower estimate for the L^2-error of the velocity and a mesh-dependent weighted L^2-error of the pressure. The global estimate for the L^2-error of the velocity is given in Section 4 and the efficiency of the global error estimator in numerical examples is demonstrated in Section 5. Section 5 additionally presents a comparison of the local a posteriori error estimator form Section 3 and the estimator in the discrete energy norm from [7] with respect to the adaptive mesh refinement.

2. The problem and mathematical preliminaries

We consider the steady state Stokes equations

$$\begin{aligned} -\Delta \boldsymbol{u} + \nabla p &= \boldsymbol{f} \quad \text{in } \Omega, \\ \nabla \cdot \boldsymbol{u} &= 0 \quad \text{in } \Omega, \\ \boldsymbol{u} &= 0 \quad \text{on } \partial\Omega \end{aligned} \tag{1}$$

in a two-dimensional domain Ω with polygonal boundary $\partial\Omega$. A weak formulation of (1) is to find $(\boldsymbol{u}, p) \in (H_0^1(\Omega))^2 \times L_0^2(\Omega)$ satisfying for all $(\boldsymbol{v}, q) \in (H_0^1(\Omega))^2 \times L_0^2(\Omega)$

$$(\nabla \boldsymbol{u}, \nabla \boldsymbol{v}) - (p, \nabla \cdot \boldsymbol{v}) + (q, \nabla \cdot \boldsymbol{u}) = (\boldsymbol{f}, \boldsymbol{v}), \tag{2}$$

where $(\cdot,\cdot)$ stands for the inner product in $(L^2(\Omega))^d$, $d = 1,2$. We assume throughout this paper the regularity

$$\boldsymbol{u} \in (H^2(\Omega))^2 \cap (H_0^1(\Omega))^2, \qquad p \in H^1(\Omega) \cap L_0^2(\Omega) \tag{3}$$

of the solution $(\boldsymbol{u}, p)$ of (1). This is given, e.g., if Ω is convex and $\boldsymbol{f} \in (L^2(\Omega))^2$.

We focus on the nonconforming P_1/P_0-finite element discretization of (2) which has been introduced by Crouzeix and Raviart [6]. Let $\mathscr{T}_h$ be a decomposition of Ω into triangles. For a given triangulation, we denote by $\{T_i\}_{i=1}^M$ the set of triangles, with $\{E_i\}_{i=1}^N$ the set of the edges of the triangles which do not belong to $\partial\Omega$, with $\{E_i\}_{i=N+1}^{N+N_D}$ the set of edges which belong to $\partial\Omega$, and with B_i the midpoint of edge E_i, $i = 1, \ldots, N + N_D$. $P_k(T)$ is the space of all polynomials defined on T

with degree not greater than k. The space of the vector valued nonconforming P_1-finite elements is defined as

$$V_h := \left\{ \begin{array}{l} \boldsymbol{v}_h \in (L^2(\Omega))^2 | \boldsymbol{v}_h|_T \in (P_1(T))^2 \ \forall T \in \mathcal{T}_h, \ \boldsymbol{v}_h \text{ is continuous} \\ \text{in } B_i, \ i = 1, \ldots, N, \text{ and } \boldsymbol{v}_h(B_i) = \boldsymbol{0}, \ i = N+1, \ldots, N+N_D. \end{array} \right\}$$

The functions of V_h are linear on each triangle, in general discontinuous across the edges, but continuous in the midpoints of the edges $\{B_i\}_{i=1}^N$. The space of piecewise constant functions in $L_0^2(\Omega)$ is denoted by Q_h:

$$Q_h := \{q_h \in L_0^2(\Omega) \,|\, q_h|_T \in P_0(T), \ \forall T \in \mathcal{T}_h\}.$$

The discrete problem is to find $(\boldsymbol{u}_h, p_h) \in V_h \times Q_h$ satisfying for all $(\boldsymbol{v}_h, q_h) \in V_h \times Q_h$

$$\sum_{T \in \mathcal{T}_h} \int_T (\nabla \boldsymbol{u}_h : \nabla \boldsymbol{v}_h - p_h \nabla \cdot \boldsymbol{v}_h + q_h \nabla \cdot \boldsymbol{u}_h) \, \mathrm{d}x = (\boldsymbol{f}, \boldsymbol{v}_h). \tag{4}$$

The norm in $(L^2(\Omega))^d$, $d = 1, 2$, is denoted by $\|\cdot\|_0$ and the seminorm in $(H^k(\Omega))^d$, $d = 1, 2$, by $|\cdot|_k$. Norms in subdomains $\omega \subset \Omega$ are indicated by an index, e.g., $\|\cdot\|_{0,\omega}$. Because we consider a nonconforming discretization, we have to introduce element-wise defined norms and seminorms for $\boldsymbol{v}_h \in V_h$

$$|\boldsymbol{v}_h|_h := \left(\sum_{T \in \mathcal{T}_h} |\boldsymbol{v}_h|_{1,T}^2 \right)^{1/2}, \quad \|\boldsymbol{v}_h\|_h := (|\boldsymbol{v}_h|_h^2 + \|\boldsymbol{v}_h\|_0^2)^{1/2}.$$

The jump $[|\boldsymbol{v}_h|]_E$ of a function $\boldsymbol{v}_h$ across an edge E is defined by

$$[|\boldsymbol{v}_h|]_E := \begin{cases} \lim_{t \to +0} \{\boldsymbol{v}_h(x + t n_E) - \boldsymbol{v}_h(x - t n_E)\}, & E \not\subset \partial\Omega \\ \lim_{t \to +0} \{-\boldsymbol{v}_h(x - t n_E)\}, & E \subset \partial\Omega \end{cases}$$

where n_E is a normal unit vector on E and $x \in E$. If $E \subset \partial\Omega$, we choose the outer normal otherwise n_E has an arbitrary but fixed orientation. With that, every edge E which separates two neighboring traingles T_1 and T_2 is associated with a uniquely oriented normal $n_E = (n_{1E}, n_{2E})$ (for definiteness from T_1 to T_2) and the jump of a function $\boldsymbol{v}_h \in V_h$ across an edge E is

$$[|\boldsymbol{v}_h|]_E = \boldsymbol{v}_h|_{T_2} - \boldsymbol{v}_h|_{T_1}.$$

We denote by $t_E = (-n_{2E}, n_{1E})$ the tangential vector on E. The functions belonging to V_h have the property

$$\int_E q[|\boldsymbol{v}_h|]_E \, \mathrm{d}s = 0 \quad \forall q \in P_0(E), \ \boldsymbol{v}_h \in V_h. \tag{5}$$

The symbol h_T stands for the diameter of the triangle T (longest edge), h_E for the length of the edge E, and ρ_T for the diameter of the largest inscribed ball of T. Positive constants which are independent of h_T and h_E are denoted by C. We shall consider uniform as well as locally refined families of triangulations $\{\mathcal{T}_h\}$ which are admissible and shape regular. Thus, we assume the existence of a constant C such that

$$\frac{h_T}{\rho_T} \leqslant C \quad \text{or} \quad \frac{h_T}{h_E} \leqslant C \quad \forall T \in \mathcal{T}_h, \ \forall E \subset \partial T.$$

Analogous to [16], we denote by ω_E the union of triangles which have the common edge E and by ω_T the union of all triangles which have a common edge with the triangle T.

We will derive in the global estimate benefit from the fact that V_h has the subspace $X_h \subset (H_0^1(\Omega))^2$ of vector valued conforming piecewise linear functions which vanish on $\partial\Omega$. We will need the standard nodal interpolation operator $R_{X_h} : (H^2(\Omega))^2 \mapsto X_h$ satisfying

$$\|\boldsymbol{v} - R_{X_h}\boldsymbol{v}\|_{0,T} \leqslant C_1 h_T^2 |\boldsymbol{v}|_{2,T} \quad \forall \boldsymbol{v} \in (H^2(T))^2, \tag{6}$$

$$\|\boldsymbol{v} - R_{X_h}\boldsymbol{v}\|_{0,E} \leqslant C_2 h_E^{3/2} |\boldsymbol{v}|_{2,T} \quad \forall \boldsymbol{v} \in (H^2(T))^2, \ E \subset \partial T \tag{7}$$

and an interpolation operator $R_{Q_h} : H^1(\Omega) \mapsto Q_h$ with the property

$$\|q - R_{Q_h} q\|_{0,T} \leqslant C_3 h_T |q|_{1,\tilde{\omega}_T} \quad \forall q \in H^1(\tilde{\omega}_T), \tag{8}$$

where $\tilde{\omega}_T$ is the set of all triangles having a common point with the triangle T. The interpolation operator of [5] fulfills (8). The constants C_1, C_2 and C_3 depend only on the smallest angle of the triangles. We set $C_I = \max\{C_1, C_2, C_3\}$.

By $\mathscr{M}_E^k : H^1(T) \mapsto P_k(E)$ the $L^2(E)$-projection onto the space of the restriction to E of all polynomials of degree k is denoted. Using the Bramble–Hilbert lemma and a scaling argument, the inequality

$$\left| \int_E u(v - \mathscr{M}_E^k v)\,\mathrm{d}s \right| \leqslant C h_T^{m+1/2} \|u\|_{0,E} |v|_{m+1,T} \tag{9}$$

with $0 \leqslant m \leqslant k$, for all elements $T \subset \omega_E$, $u \in L^2(E)$, and $v \in H^{m+1}(T)$ can be proven [12].

In the following, we need local inverse estimates of seminorms of polynomials in Sobolev spaces

$$\begin{aligned} |v|_{m,p,T} &\leqslant C h_T^{-1} |v|_{m-1,p,T} && \forall v\colon\ v|_T \in P_k(T), \\ \sum_{T \subset \omega_E} |v|_{m,p,T} &\leqslant C h_E^{-1} \sum_{T \subset \omega_E} |v|_{m-1,p,T} && \forall v\colon\ v|_T \in P_k(T),\ \forall T \subset \omega_E, \end{aligned} \tag{10}$$

for $m \geqslant 1$, $p \in [1, \infty]$. The proof follows the lines of [4, Theorem 17.2], using the shape regularity of the triangulation in the second estimate.

3. A local lower error bound

We define the residual-based local a posteriori error estimator $\forall \boldsymbol{v}_h \in V_h$

$$\eta_T^2 := h_T^4 \|\boldsymbol{f}_h\|_{0,T}^2 + h_T^2 \|\nabla \cdot \boldsymbol{v}_h\|_{0,T}^2 + \sum_{\substack{E \subset \partial T \\ E \not\subset \partial\Omega}} h_E^3 \|[|\nabla \boldsymbol{v}_h \cdot n_E - q_h I n_E|]_E\|_{0,E}^2 + \sum_{E \subset \partial T} h_E \|[|\boldsymbol{v}_h|]_E\|_{0,E}^2 \tag{11}$$

where $\boldsymbol{f}_h$ is a polynomial approximation of $\boldsymbol{f}$ of fixed degree. The 2×2 identity matrix is denoted by I. The first and second term of η_T are norms of element residuals of the strong formulation of the equation of momentum and mass, respectively. These terms can be found in a posteriori error estimators for conforming finite element discretizations as well as the third term which often is called edge residual. Finally, the last term gives information on the nonconformity of $\boldsymbol{v}_h$. The jump of the tangential derivatives across the edges may replace the jumps of the nonconforming function in η_T because of

$$\|[|\boldsymbol{v}_h|]_E\|_{0,E}^2 = \frac{h_E^2}{12}\left\|\left[\left|\frac{\partial \boldsymbol{v}_h}{\partial t_E}\right|\right]_E\right\|_{0,E}^2 \qquad \forall \boldsymbol{v}_h \in V_h.$$

In this section, we investigate if η_T can be used as local error estimator for adaptive grid refinement. Therefore, it will be shown that η_T gives a local lower bound on the error in the L^2-norm of the velocity and the weighted mesh-dependent L^2-norm of the pressure. However, the estimate of the jump terms of the nonconforming function leads to an additional term in the error estimate. The local lower bound holds for each pair of discrete functions since the solution of the discrete problem (4) does not play any rôle in the proof of Theorem 1.

Theorem 1. *Let* $(\boldsymbol{u}, p)$ *be the solution of* (1) *with the regularity given by* (3). *Given a shape regular family of triangulations and a fixed polynomial degree of the approximation* $\boldsymbol{f}_h$ *of* $\boldsymbol{f}$, *then for all pairs of functions* $(\boldsymbol{v}_h, q_h) \in V_h \times Q_h$ *satisfying*

$$\|\boldsymbol{f} - \boldsymbol{f}_h\|_{0,\omega_T} = \mathcal{O}((\|\boldsymbol{u} - \boldsymbol{v}_h\|_{0,\omega_T}^2 + h_T^2\|p - q_h\|_{0,\omega_T}^2)^{1/2})$$

there is a constant C *such that*

$$\eta_T \leqslant C(\|\boldsymbol{u} - \boldsymbol{v}_h\|_{0,\omega_T}^2 + h_T^2\|p - q_h\|_{0,\omega_T}^2)^{1/2} + Ch_T^2|\boldsymbol{u}|_{2,\omega_T}$$
$$+ \mathcal{O}(h_T^2(\|\boldsymbol{u} - \boldsymbol{v}_h\|_{0,\omega_T}^2 + h_T^2\|p - q_h\|_{0,\omega_T}^2)^{1/2})$$

for all triangles T.

The remainder of this section is devoted to the proof of Theorem 1. Each term of η_T will be estimated separately from above by the local error.

A standard tool for proving local a posteriori error estimates are cutoff functions, see, e.g., [15, 16]. Often, the use of appropriate cutoff functions is the key to obtain local error bounds, e.g., for robust error estimators in convection dominated problems [17, 18]. The special cutoff function B_E, defined below, will play an essential rôle for the nonconforming discretization.

Let $T \in \mathcal{T}_h$ be an arbitrary triangle and $E \subset \partial T$. We denote by λ_E the linear function which is zero on E and 1 in the corner of T opposite to E. In contrast to the derivation of a posteriori error estimates in the discrete energy norm, we need in the following cutoff functions which belong to $C^1(\bar{\Omega})$. We define for each triangle T the element bubble function

$$\mathrm{B}_T = \begin{cases} (27\lambda_{E_1}\lambda_{E_2}\lambda_{E_3})^2 & \text{in } T, \\ 0 & \text{otherwise}, \end{cases} \tag{12}$$

where E_1, E_2, E_3 are the edges of T. Next, we construct an edge bubble function B_E with $\operatorname{supp} \mathrm{B}_E = \omega_E$, see Fig. 1. Let E be the common edge of the triangles T_1 and T_2. The other edges of T_1 are E_1 and E_2. The triangle T_1 is reflected on E with the images E_1^* and E_2^* of E_1 and E_2, respectively.

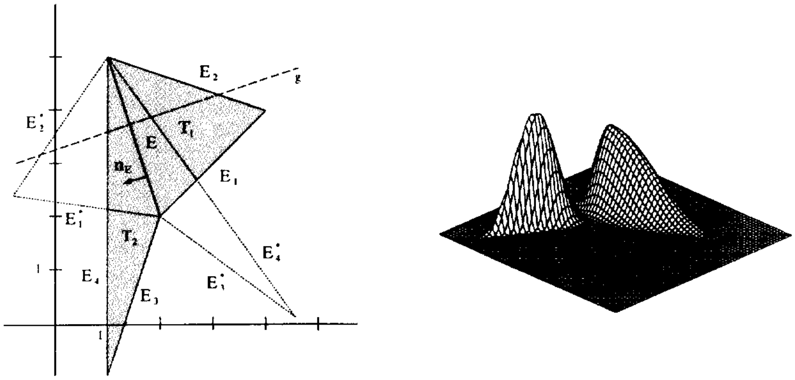

Fig. 1. Cutoff function B_E.

In the same way, we obtain E_3^* and E_4^* by reflecting T_2 on E. We define

$$B_E = \begin{cases} 256\lambda_{E_1}^2\lambda_{E_2}^2\lambda_{E_1^*}^2\lambda_{E_2^*}^2 & \text{on } T_1, \\ 256\lambda_{E_3}^2\lambda_{E_4}^2\lambda_{E_3^*}^2\lambda_{E_4^*}^2 & \text{on } T_2, \\ 0 & \text{otherwise.} \end{cases} \tag{13}$$

Some properties of the cutoff functions B_T and B_E are summarized in

Lemma 2. *The cutoff functions given in* (12) *and* (13) *have the following properties*:

$$B_T, B_E \in C^1(\bar{\Omega}), \quad B_T|_T \in P_6(T), \; B_E|_T \in P_8(T) \quad \forall T \subset \omega_E, \quad 0 \leqslant B_T, \; B_E \leqslant 1, \tag{14a}$$

$$\begin{aligned} &B_T = 0 \quad \text{on } \partial T, \qquad \nabla B_T = \mathbf{0} \quad \text{on } \partial T, \\ &B_E = 0 \quad \text{on } \partial\omega_E, \quad \nabla B_E = \mathbf{0} \quad \text{on } \partial\omega_E. \end{aligned} \tag{14b}$$

B_E is continuous on E and

$$\nabla B_E \cdot n_E = 0 \quad \text{on } E. \tag{15}$$

Proof. The first and second property, (14a) and (14b), follow directly from the definition of the cutoff functions. Property (15) follows from

$$\lambda_{E_1}|_E = \lambda_{E_1^*}|_E = \lambda_{E_3}|_E = \lambda_{E_3^*}|_E \quad \text{and} \quad \lambda_{E_2}|_E = \lambda_{E_2^*}|_E = \lambda_{E_4}|_E = \lambda_{E_4^*}|_E.$$

With that, we find $B_E|_E = 256\lambda_{E_1}^4\lambda_{E_2}^4$. Finally, (15) can be proven considering an arbitrary line g across E and perpendicular to E. The definition of B_E on T_1 is continued to the mirror image of T_1. In this way, a function on g is defined which is continuously differentiable and symmetric with respect to E. Thus, we have $\nabla B_E \cdot n_E = 0$ in the cross point of g and E. □

In the following, we need uniform norm equivalences of weighted L^2-norms in finite dimensional spaces. The proofs follow the lines of Lemma 3.3 in [16] using the equivalence of norms in finite dimensional spaces, the boundedness of the cutoff functions and scaling arguments.

Lemma 3. *The cutoff functions defined in* (12) *and* (13) *satisfy the following inequalities*:

$$\|v\|_{0,T}^2 \leqslant C \int_T v^2 \mathrm{B}_T \,\mathrm{d}x \quad \forall v \in P_k(T), \tag{16}$$

$$\|v\|_{0,E}^2 \leqslant C \int_E v^2 \mathrm{B}_E \,\mathrm{d}x \quad \forall v \in P_k(E), \tag{17}$$

$$\|v\mathrm{B}_T\|_{0,T} \leqslant \|v\|_{0,T} \quad \forall v \in P_k(T), \tag{18}$$

$$\|v\mathrm{B}_E\|_{0,\omega_E} \leqslant \|v\|_{0,\omega_E} \quad \forall v \text{ with } v|_{T_i} \in P_k(T_i), T_i \subset \omega_E, \tag{19}$$

where C is a constant independent of T and h_T. In (16) *and* (17), *C depends on k.*

The residual of the equation of mass will be estimated in the following lemma.

Lemma 4. *Let $(\boldsymbol{u}, p)$ be the solution of* (1) *and $\boldsymbol{v}_h \in V_h$ an arbitrary function. Then, there is a constant C such that for each element T of the shape regular family of triangulations $\{\mathscr{T}_h\}$, the estimate*

$$h_T \|\nabla \cdot \boldsymbol{v}_h\|_{0,T} \leqslant C \|\boldsymbol{u} - \boldsymbol{v}_h\|_{0,T}$$

is valid.

Proof. Using (16), $\nabla \cdot \boldsymbol{u} = 0$, integration by parts and (14), we obtain

$$\begin{aligned}\|\nabla \cdot \boldsymbol{v}_h\|_{0,T}^2 &\leqslant C \int_T \nabla \cdot (\boldsymbol{v}_h - \boldsymbol{u})(\nabla \cdot \boldsymbol{v}_h \mathrm{B}_T)\,\mathrm{d}x \\ &= C \int_T (\boldsymbol{u} - \boldsymbol{v}_h) \cdot \nabla(\nabla \cdot \boldsymbol{v}_h \mathrm{B}_T)\,\mathrm{d}x.\end{aligned}$$

Applying the Cauchy–Schwarz inequality, the inverse estimate (10) and (18), we get

$$\|\nabla \cdot \boldsymbol{v}_h\|_{0,T}^2 \leqslant C h_T^{-1} \|\boldsymbol{u} - \boldsymbol{v}_h\|_{0,T} \|\nabla \cdot \boldsymbol{v}_h\|_{0,T}. \qquad \square$$

We will estimate the norm of the residual of the equation describing the conservation of momentum in the following lemma.

Lemma 5. *Let $(\boldsymbol{u}, p)$ be the solution of* (1) *and $(\boldsymbol{v}_h, q_h) \in V_h \times Q_h$ an arbitrary pair of functions. Assuming the regularity of the solution given by* (3), *then there is a constant C such that*

$$h_T^2 \|\boldsymbol{f}_h\|_{0,T} \leqslant C[\|\boldsymbol{u} - \boldsymbol{v}_h\|_{0,T} + h_T \|p - q_h\|_{0,T} + h_T^2 \|\boldsymbol{f} - \boldsymbol{f}_h\|_{0,T}] \tag{20}$$

for each T of a shape regular family of triangulations.

Proof. Let T be an arbitrary triangle. Using (16), (1) and $\Delta \boldsymbol{v}_h|_T = 0$, $\nabla q_h|_T = 0$, $\forall (\boldsymbol{v}_h, q_h) \in V_h \times Q_h$, we get

$$\|\boldsymbol{f}_h\|_{0,T}^2 \leqslant C \int_T (-\Delta(\boldsymbol{u} - \boldsymbol{v}_h) + \nabla(p - q_h))\boldsymbol{f}_h \mathrm{B}_T + (\boldsymbol{f}_h - \boldsymbol{f})\boldsymbol{f}_h \mathrm{B}_T \,\mathrm{d}x.$$

Now, integration by parts and (14) yield

$$\|f_h\|_{0,T}^2 \leqslant C\int_T -(\boldsymbol{u}-\boldsymbol{v}_h)\Delta(f_h\mathrm{B}_T)-(p-q_h)\nabla\cdot(f_h\mathrm{B}_T)+(f_h-f)f_h\mathrm{B}_T\,\mathrm{d}x.$$

All terms can be estimated using the Cauchy–Schwarz inequality, the inverse estimate (10), and (18) which yields (20). □

The edge residual is estimated in a similar way using the cutoff function B_E. The smoothness of B_E plays an essential rôle for the following estimate. Integrating by parts in ω_E, we obtain a line integral on the edge E which vanishes because of $\nabla\mathrm{B}_E\cdot n_E=0$ on E.

Lemma 6. *With the assumptions of Lemma 5, there is a constant C such that*

$$\begin{aligned}&h_E^{3/2}\|[|\nabla\boldsymbol{v}_h\cdot n_E-q_hIn_E|]_E\|_{0,E}\\&\quad\leqslant C[\|\boldsymbol{u}-\boldsymbol{v}_h\|_{0,\omega_E}+h_E\|p-q_h\|_{0,\omega_E}+h_E^2\|f-f_h\|_{0,\omega_E}]\end{aligned}$$

for all edges E with $E\not\subset\partial\Omega$.

Proof. Before starting the estimate, we note that $[|\nabla\boldsymbol{v}_h\cdot n_E-q_hIn_E|]_E$ is a constant vector valued function on each edge E. Let us denote with $[|\nabla\boldsymbol{v}_h\cdot n_E-q_hIn_E|]_E^C$ the constant continuation of $[|\nabla\boldsymbol{v}_h\cdot n_E-q_hIn_E|]_E$ to ω_E. Then, taking into consideration the regularity of the triangulation, we have the estimate

$$\|[|\nabla\boldsymbol{v}_h\cdot n_E-q_hIn_E|]_E^C\|_{0,\omega_E}\leqslant Ch_E^{1/2}\|[|\nabla\boldsymbol{v}_h\cdot n_E-q_hIn_E|]_E\|_{0,E}. \tag{21}$$

Now, using (17), element-wise integration by parts and (14), we obtain

$$\begin{aligned}&\|[|\nabla\boldsymbol{v}_h\cdot n_E-q_hIn_E|]_E\|_{0,E}^2\\&\quad\leqslant C\sum_{T\subset\omega_E}\left[\int_T\nabla(\boldsymbol{u}-\boldsymbol{v}_h):\nabla([|\nabla\boldsymbol{v}_h\cdot n_E-q_hIn_E|]_E^C\mathrm{B}_E)\,\mathrm{d}x\right.\\&\qquad-\int_T(p-q_h)\nabla\cdot([|\nabla\boldsymbol{v}_h\cdot n_E-q_hIn_E|]_E^C\mathrm{B}_E)\,\mathrm{d}x\\&\qquad\left.+\int_T(\Delta(\boldsymbol{u}-\boldsymbol{v}_h)-\nabla(p-q_h))\cdot[|\nabla\boldsymbol{v}_h\cdot n_E-q_hIn_E|]_E^C\mathrm{B}_E\,\mathrm{d}x\right].\end{aligned}$$

Integrals on E containing jumps of $\nabla\boldsymbol{u}$ and p vanish since these functions are continuous almost everywhere. In the following, we estimate each term separately. The first term is integrated by parts once more. Using (14), we get

$$\begin{aligned}&\sum_{T\subset\omega_E}\int_T\nabla(\boldsymbol{u}-\boldsymbol{v}_h):\nabla([|\nabla\boldsymbol{v}_h\cdot n_E-q_hIn_E|]_E^C\,\mathrm{B}_E)\,\mathrm{d}x\\&\quad=-\int_{\omega_E}(\boldsymbol{u}-\boldsymbol{v}_h)([|\nabla\boldsymbol{v}_h\cdot n_E-q_hIn_E|]_E^C\Delta\mathrm{B}_E)\,\mathrm{d}x\\&\qquad+\int_E[|\boldsymbol{v}_h|]_E\cdot[|\nabla\boldsymbol{v}_h\cdot n_E-q_hIn_E|]_E(\nabla\mathrm{B}_E\cdot n_E)\,\mathrm{d}s.\end{aligned}$$

The integral on the edge E vanishes because of (15). With the inverse inequality (10), (19) and (21), we obtain

$$\sum_{T\subset\omega_E}\int_T \nabla(\boldsymbol{u}-\boldsymbol{v}_h)\cdot[|\nabla\boldsymbol{v}_h\cdot\boldsymbol{n}_E-q_hI\boldsymbol{n}_E|]_E^C\,\mathrm{B}_E\,\mathrm{d}x$$
$$\leqslant Ch_E^{-3/2}\|\boldsymbol{u}-\boldsymbol{v}_h\|_{0,\omega_E}\|[|\nabla\boldsymbol{v}_h\cdot\boldsymbol{n}_E-q_hI\boldsymbol{n}_E|]_E\|_{0,E}.$$

The second term is estimated in the same way. We can write the third term, using $\Delta(\boldsymbol{u}-\boldsymbol{v}_h)-\nabla(p-q_h)=-\boldsymbol{f}$ on T, in the form

$$-\sum_{T\subset\omega_E}\int_T \boldsymbol{f}_h\cdot[|\nabla\boldsymbol{v}_h\cdot\boldsymbol{n}_E-q_hI\boldsymbol{n}_E|]_E^C\,\mathrm{B}_E\,\mathrm{d}x$$
$$-\sum_{T\subset\omega_E}\int_T(\boldsymbol{f}-\boldsymbol{f}_h)\cdot[|\nabla\boldsymbol{v}_h\cdot\boldsymbol{n}_E-q_hI\boldsymbol{n}_E|]_E^C\,\mathrm{B}_E\,\mathrm{d}x.$$

These terms can be estimated using the Cauchy–Schwarz inequality, (19), (21) and the estimate (20) for $\|\boldsymbol{f}_h\|_{0,T}$. The combination of all estimates proves the lemma. □

Finally, we consider the term of the error estimator which gives information about the nonconformity of the discrete function.

Lemma 7. *Given a shape regular family of triangulations, there is a positive constant C such that for each edge E,* $\forall\boldsymbol{v}\in(H^2(\omega_E))^2$, $\forall\boldsymbol{v}_h\in V_h$

$$h_E^{1/2}\|[|\boldsymbol{v}_h|]_E\|_{0,E}\leqslant C(\|\boldsymbol{v}-\boldsymbol{v}_h\|_{0,\omega_E}+h_E^2|\boldsymbol{v}|_{2,\omega_E}). \tag{22}$$

Proof. Let $R_{X_h}\boldsymbol{v}\in X_h$ be the interpolant of $\boldsymbol{v}$ and $\omega_E=T_1\cup T_2$. Using a standard estimate of the trace of a polynomial from $P_k(T)$ and (6), we get

$$\|[|\boldsymbol{v}_h|]_E\|_{0,E}^2=\int_E[(\boldsymbol{v}_h-R_{X_h}\boldsymbol{v})|_{T_1}-(\boldsymbol{v}_h-R_{X_h}\boldsymbol{v})|_{T_2}]^2\,\mathrm{d}s$$
$$\leqslant 2\left\{\int_E[(\boldsymbol{v}_h-R_{X_h}\boldsymbol{v})|_{T_1}]^2+\int_E[(\boldsymbol{v}_h-R_{X_h}\boldsymbol{v})|_{T_2}]^2\right\}$$
$$\leqslant C(h_E^{-1}\|\boldsymbol{v}-\boldsymbol{v}_h\|_{0,\omega_E}^2+h_E^3|\boldsymbol{v}|_{2,\omega_E}^2).\qquad\square$$

Remark 8. An estimate of the form $h_E^{1/2}\|[|\boldsymbol{v}_h|]_E\|_{0,E}\leqslant C\|\boldsymbol{v}-\boldsymbol{v}_h\|_{0,\omega_E}$ would be desirable. However, such an estimate is not in general true. We consider the union ω_E of two triangles shown in Fig. 2. The variable perpendicular to E in the direction of $\boldsymbol{n}_E$ is denoted by x. Given an arbitrary function $\boldsymbol{v}_h\in V_h$ with $\boldsymbol{v}_h(\mathrm{B}_E)=\boldsymbol{0}$, $\|[|\boldsymbol{v}_h|]_E\|_{0,E}=C>0$, the left-hand side of (22) is a fixed positive number.

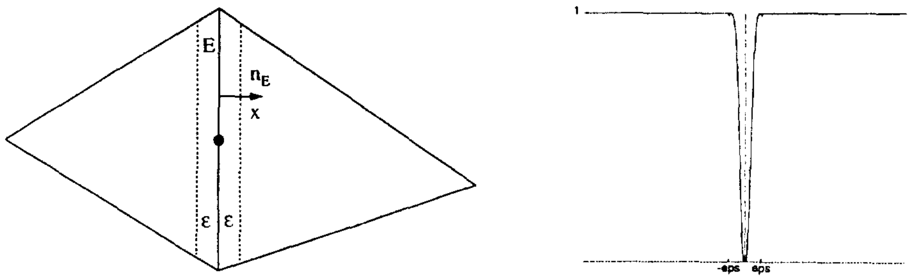

Fig. 2. ω_E (left) and $\phi_E(x)$ (right).

Now, defining $\boldsymbol{v}_\varepsilon = \boldsymbol{v}_h \phi_E$ with

$$\phi_E(x) = \begin{cases} 1 & x \geqslant \varepsilon, \\ \left(1 - \left(\dfrac{x}{\varepsilon} - 1\right)^4\right)^4 & x \in [0, \varepsilon), \\ \left(-1 + \left(\dfrac{x}{\varepsilon} + 1\right)^4\right)^4 & x \in (-\varepsilon, 0), \\ 1 & x \leqslant -\varepsilon, \end{cases}$$

see Fig. 2, we find $\boldsymbol{v}_\varepsilon \in (H^2(\omega_E))^2$ and $\|\boldsymbol{v}_\varepsilon - \boldsymbol{v}_h\|_{0,\omega_E} \to 0$ for $\varepsilon \to 0$.

4. Global a posteriori estimate for the L^2-error of the velocity

We apply a technique developed by Johnson et al., see, e.g., [10]. It consists of four steps:
1. error representation with the solution of a continuous dual problem,
2. Galerkin orthogonality of the discretization,
3. interpolation estimates for the solution of the dual problem,
4. strong stability of the dual problem.

Let $(\boldsymbol{u}_h, p_h)$ be the solution of the discrete problem (4). The strong formulation of the continuous dual problem with the error $\boldsymbol{u} - \boldsymbol{u}_h$ as right-hand side is

$$\begin{aligned} -\Delta \boldsymbol{z} - \nabla s &= \boldsymbol{u} - \boldsymbol{u}_h && \text{in } \Omega, \\ \nabla \cdot \boldsymbol{z} &= 0 && \text{in } \Omega, \\ \boldsymbol{z} &= \boldsymbol{0} && \text{on } \partial\Omega. \end{aligned} \tag{23}$$

For the solution $(\boldsymbol{z}, s)$ of the corresponding weak problem, we require the regularity

$$(\boldsymbol{z}, s) \in (H^2(\Omega) \cap H_0^1(\Omega))^2 \times (H^1(\Omega) \cap L_0^2(\Omega)) \tag{24}$$

and the stability

$$|\boldsymbol{z}|_2 + |s|_1 \leqslant C_S \|\boldsymbol{u} - \boldsymbol{u}_h\|_0. \tag{25}$$

The following theorem gives the estimate of the global L^2-error of the velocity.

Theorem 9. *Let* $(\boldsymbol{u}, p)$ *be the solution of* (1) *with the regularity given by* (3) *and* $(\boldsymbol{u}_h, p_h)$ *the solution of* (4). *For the solution* $(\boldsymbol{z}, s)$ *of the dual problem* (23), *we assume the regularity given by* (24) *and the stability* (25). *Then, for a shape regular family of triangulations, there is a constant* $C = C(C_I C_S)$ *such that the global error estimate*

$$\|\boldsymbol{u}-\boldsymbol{u}_h\|_0 \leqslant C\eta + C\left(\sum_{T\in\mathcal{T}_h} h_T^4 \|\boldsymbol{f}-\boldsymbol{f}_h\|_{0,T}^2\right)^{1/2}$$

holds with

$$\eta = \left(\sum_{T\in\mathcal{T}_h}\left(h_T^4\|\boldsymbol{f}_h\|_{0,T}^2 + h_T^2\|\nabla\cdot\boldsymbol{u}_h\|_{0,T}^2\right) + \sum_{\substack{E\subset\partial T\\ E\not\subset\partial\Omega}} h_E^3 \|[|\nabla \boldsymbol{u}_h\cdot \boldsymbol{n}_E - p_h I \boldsymbol{n}_E|]_E\|_{0,E}^2 + \sum_{E\subset\partial T} h_E \|[|\boldsymbol{u}_h|]_E\|_{0,E}^2\right)^{1/2}. \tag{26}$$

Here, C_I *is defined in* (6)–(8), *and* $\boldsymbol{f}_h$ *is a polynomial approximation on* $\boldsymbol{f}$ *of fixed degree.*

Proof. We start by testing the dual problem (23) with $\boldsymbol{u}-\boldsymbol{u}_h$ and integrating by parts. Using the error $p-p_h$ as test function from Q, we obtain

$$\|\boldsymbol{u}-\boldsymbol{u}_h\|_0^2 = \sum_{T\in\mathcal{T}_h}\left[\int_T \nabla\boldsymbol{z}\cdot\nabla(\boldsymbol{u}-\boldsymbol{u}_h) + s\nabla\cdot(\boldsymbol{u}-\boldsymbol{u}_h) - (p-p_h)\nabla\cdot\boldsymbol{z}\,\mathrm{d}x + \sum_{E\subset\partial T}\int_E (\nabla\boldsymbol{z}\cdot\boldsymbol{n}_E)\cdot\boldsymbol{u}_h + s(\boldsymbol{u}_h\cdot\boldsymbol{n}_E)\,\mathrm{d}s\right]. \tag{27}$$

Since $X_h \subset V_h$, we get with (2) the Galerkin orthogonality

$$0 = \sum_{T\in\mathcal{T}_h}\left[\int_T \nabla(\boldsymbol{u}-\boldsymbol{u}_h) : \nabla\boldsymbol{v}_h - (p-p_h)\nabla\cdot\boldsymbol{v}_h + q_h\nabla\cdot(\boldsymbol{u}-\boldsymbol{u}_h)\,\mathrm{d}x\right]$$

for all $(\boldsymbol{v}_h, q_h)\in X_h\times Q_h$. Choosing $\boldsymbol{v}_h = R_{X_h}\boldsymbol{z} = \boldsymbol{z}_h$ and $q_h = R_{Q_h}s = s_h$, adding these to (27), and integrating by parts give

$$\begin{aligned}
&\|\boldsymbol{u}-\boldsymbol{u}_h\|_0^2\\
&\quad= \sum_{T\in\mathcal{T}_h}\left[\int_T(-\Delta(\boldsymbol{u}-\boldsymbol{u}_h) + \nabla(p-p_h))\cdot(\boldsymbol{z}-\boldsymbol{z}_h) + (s-s_h)\nabla\cdot(\boldsymbol{u}-\boldsymbol{u}_h)\,\mathrm{d}x\right.\\
&\qquad\left. + \sum_{E\subset\partial T}\int_E(\nabla(\boldsymbol{u}-\boldsymbol{u}_h)\cdot\boldsymbol{n}_E - (p-p_h)\boldsymbol{n}_E)\cdot(\boldsymbol{z}-\boldsymbol{z}_h) + (\nabla\boldsymbol{z}\cdot\boldsymbol{n}_E)\cdot\boldsymbol{u}_h + s(\boldsymbol{u}_h\cdot\boldsymbol{n}_E)\,\mathrm{d}s\right].
\end{aligned}$$

The estimate of the first terms is standard [10]. Using the interpolation estimates (6)–(8) and the stability of the dual problem (25) gives the first three terms of the error estimator.

The terms coming from the nonconformity of $\boldsymbol{u}_h$ are estimated using (5), (9), and (25):

$$\begin{aligned}
\sum_{T\in\mathcal{T}_h}\sum_{E\subset\partial T}\int_E(\nabla \boldsymbol{z}\cdot\boldsymbol{n}_E)\cdot\boldsymbol{u}_h\,\mathrm{d}s &\leqslant \sum_E\left|\int_E(\nabla \boldsymbol{z}\cdot\boldsymbol{n}_E)\cdot[|\boldsymbol{u}|]_E\,\mathrm{d}s\right|\\
&= \sum_E\left|\int_E((\nabla \boldsymbol{z}-\mathcal{M}_E^0(\nabla \boldsymbol{z}))\cdot\boldsymbol{n}_E)\cdot[|\boldsymbol{u}_h|]_E\,\mathrm{d}s\right|\\
&\leqslant C\sum_E h_E^{1/2}\|[|\boldsymbol{u}_h|]_E\|_{0,E}|\nabla \boldsymbol{z}\cdot\boldsymbol{n}_E|_{1,\omega_E}\\
&\leqslant C\,C_S\left(\sum_E h_E\|[|\boldsymbol{u}_h|]_E\|_{0,E}^2\right)^{1/2}\|\boldsymbol{u}-\boldsymbol{u}_h\|_0,\\
\sum_{T\in\mathcal{T}_h}\sum_{E\subset\partial T}\int_E s(\boldsymbol{u}_h\cdot\boldsymbol{n}_E)\,\mathrm{d}s &\leqslant \sum_E\left|\int_E(s-\mathcal{M}_E^0(s))[|\boldsymbol{u}_h|]_E\cdot\boldsymbol{n}_E\,\mathrm{d}s\right|\\
&\leqslant C\sum_E h_E^{1/2}\|[|\boldsymbol{u}_h|]_E\cdot\boldsymbol{n}_E\|_{0,E}|s|_{1,\omega_E}\\
&\leqslant C\,C_S\left(\sum_E h_E\|[|\boldsymbol{u}_h|]_E\|_{0,E}^2\right)^{1/2}\|\boldsymbol{u}-\boldsymbol{u}_h\|_0. \qquad\square
\end{aligned}$$

Errors coming from numerical integration in assembling the right-hand side of the discrete system (4) and from the termination of the iterative solver at an approximation of the solution of the discrete system violate the Galerkin orthogonality and result in additional terms in the global error estimate. These terms will be considered as of higher order in the numerical practice. To justify this, it is necessary that in the computation of the error estimator η at least a good approximation of $(\boldsymbol{u}_h, p_h)$ is used.

In the proof of Theorem 9, we do not need a solution of a discrete problem belonging to the dual problem (23) but only an interpolant $\boldsymbol{z}_h$ of $\boldsymbol{z}$. We make use of the fact that V_h contains the conform subspace X_h so that we can choose $\boldsymbol{z}_h\in X_h$. Thus, line integrals for the reason of discontinuities of $\boldsymbol{z}_h$ do not occur in the following integration by parts. So to speak, the dual problem is treated in a conforming way.

The analysis of Sections 3 and 4 can be extended to inhomogeneous Dirichlet boundary conditions and Neumann boundary conditions, in a way analogous to [7, 8].

5. Numerical results

In this section, we present numerical results which demonstrate the efficiency of the global error estimator η and we give a comparison of the adaptive mesh refinement using the local error estimator η_T (11) and a local estimator of the error in the discrete energy norm

$$(|\boldsymbol{u}-\boldsymbol{u}_h|_h^2+\|p-p_h\|_0^2)^{1/2}$$

proposed by Dari et al. [7]. The global error estimator η is said to be *efficient* if there are constants $0 < c_0 < c_1$ such that for all triangulations $\mathscr{T}_h$

$$c_0 \leqslant \frac{\eta}{\|\boldsymbol{u}-\boldsymbol{u}_h\|_0} \leqslant c_1.$$

Example 10. First, we consider an example with a smooth solution satisfying the regularity assumptions (3). The right-hand side is chosen such that

$$\boldsymbol{u} = \operatorname{curl} \Psi, \quad \Psi = x^2y^2(1-x)^2(1-y)^2, \quad p = x^3 + y^3 - 0.5$$

is the solution of (1) in $\Omega = [0,1]\times[0,1]$.

We have performed computations using different coarse grids and uniform refinement. For some tests, the exact and the estimated error in the L^2-norm of the velocity are presented in Fig. 3 together with the corresponding coarse grids. In each test, the ratio of the exact and estimated error has been nearly constant on all levels which demonstrates the efficiency of the error estimator.

Example 11. The following example has been used in [3, 16] for testing a posteriori error estimators for the error in the energy norm and for conforming finite element discretizations.

Let Ω be the disc with the center $(0,0)$ and the radius 1 which has a crack along the x-axis between the points $(0,0)$ and $(1,0)$, see Fig. 4. We consider the Stokes equations

$$\begin{array}{ll} -\Delta \boldsymbol{u} + \nabla p = \boldsymbol{0} & \text{in } \Omega, \\ \nabla\cdot\boldsymbol{u} = 0 & \text{in } \Omega, \\ \boldsymbol{u} = \boldsymbol{g} & \text{on } \partial\Omega, \end{array} \tag{28}$$

where the boundary condition is chosen such that

$$\boldsymbol{u} = \frac{3}{2}\sqrt{r}\left(\cos\frac{\theta}{2} - \cos\frac{3\theta}{2}, 3\sin\frac{\theta}{2} - \sin\frac{3\theta}{2}\right), \quad p = -\frac{6}{\sqrt{r}}\cos\frac{\theta}{2}$$

with $r^2 = x^2 + y^2$ and $0 \leqslant \theta \leqslant 2\pi$ is the exact solution of (28), see Fig. 5. The solution has a singularity in the origin, it is $\boldsymbol{u} \notin (H^2(\Omega))^2$ and $p \notin H^1(\Omega)$. Thus, the theoretical assumptions of Sections 3 and 4 are not fulfilled. As criteria for the quality of the computed solution $(\boldsymbol{u}_h, p_h)$, we have chosen $\|\boldsymbol{u}-\boldsymbol{u}_h\|_0$ and the resolution of the singularity of the pressure. This resolution is measured with the minimal value $p_{h,\min}$ and the maximal value $p_{h,\max}$ of p_h. The coarsest grid is presented in Fig. 4.

Besides the local error estimator η_T, we have applied for the adaptive grid refinement the local error estimator in the discrete energy norm

$$\eta_{T,\mathrm{eng}}^2 := h_T^2\|\boldsymbol{f}_h\|_{0,T}^2 + \|\nabla\cdot\boldsymbol{u}_h\|_{0,T}^2 + \sum_{\substack{E\subset\partial T\\ E\not\subset\partial\Omega}} h_E\|[|\nu\nabla\boldsymbol{u}_h\cdot\boldsymbol{n}_E - p_h I\boldsymbol{n}_E|]_E\|_{0,E}^2 + \sum_{E\subset\partial T} h_E^{-1}\|[|\boldsymbol{u}_h|]_E\|_{0,E}^2$$

proposed by Dari et al. [7]. For the adaptive grid refinement criteria have to be set for choosing elements for refinement or coarsening, tolerances for these criteria, a minimal amount of refinement,

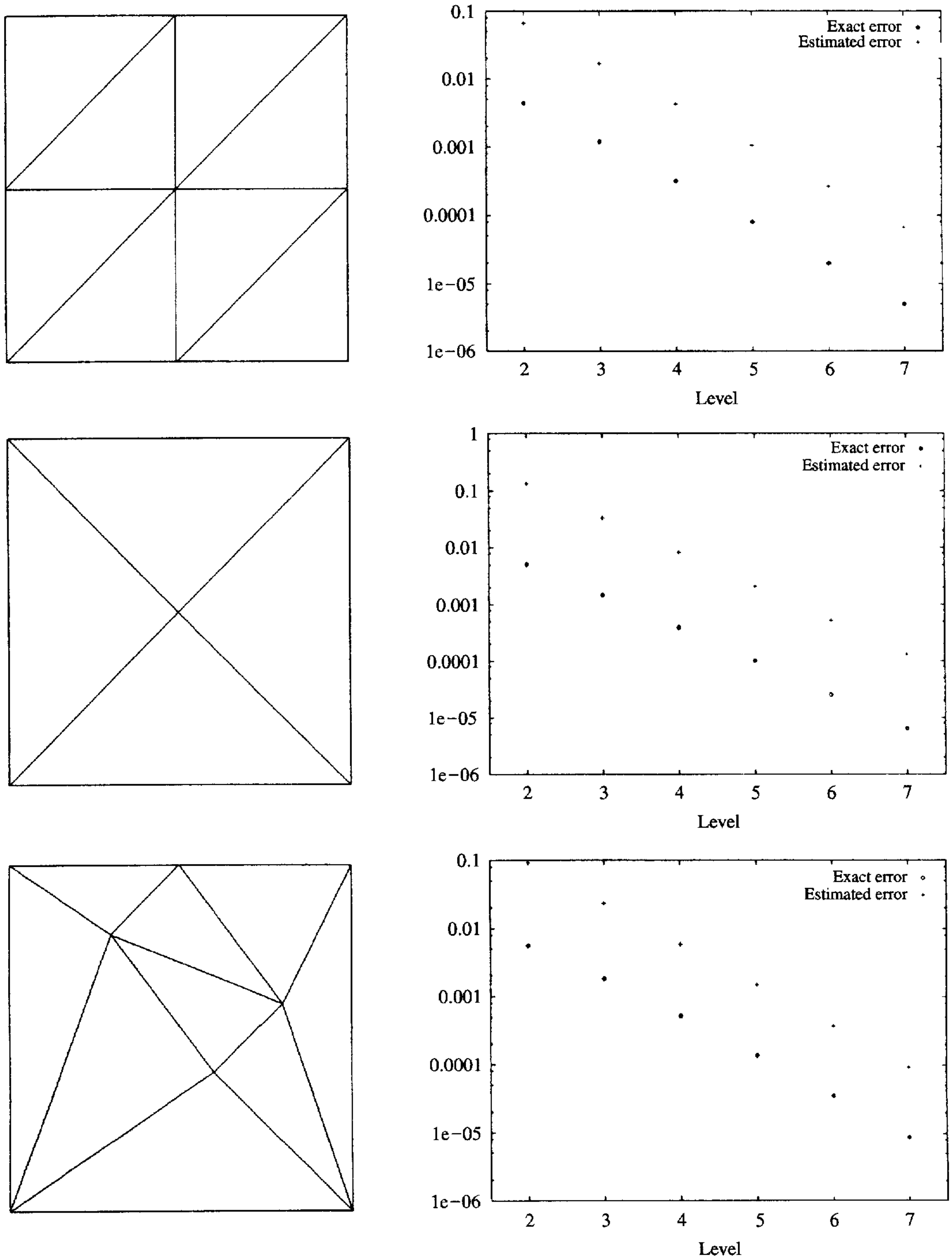

Fig. 3. Example 10, coarse grids (level 0), exact and estimated errors.

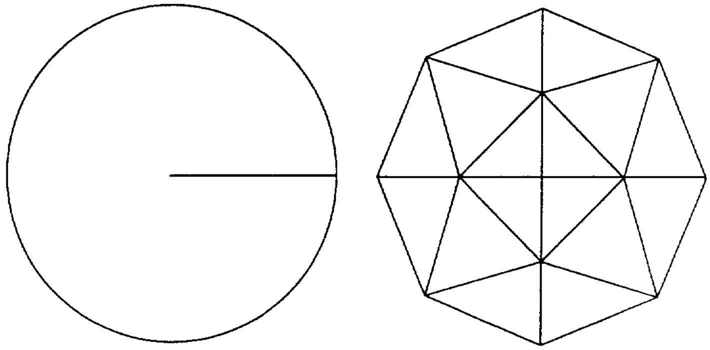

Fig. 4. Domain and coarsest grid (level 0) for Example 11.

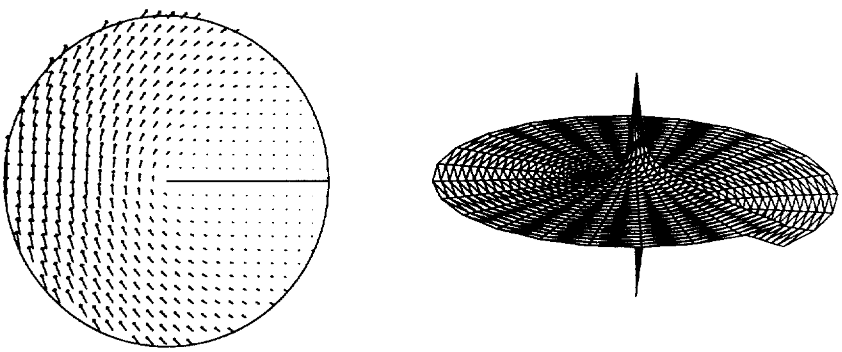

Fig. 5. Solution (velocity and pressure) of Example 11.

and a starting point for the adaptive refinement process. For details on these subjects see [11]. The sequence

assemble $\rightarrow$ solve $\rightarrow$ estimate the error $\rightarrow$ refine $\rightarrow$ interpolate

is called a *step*.

The results of the numerical tests are presented in Table 1. The use of both types of local error estimators leads to much better results than uniform refinement. Only 1.5% of the degrees of freedom are necessary to achieve similar results on the locally refined meshes of $\eta_{T,\text{eng}}$ (step 9) like with uniform refinement (step 7). The local a posteriori error estimator $\eta_{T,\text{eng}}$ refines above all at the singularity whereas the local refinement produced by η_T covers a larger domain, compare Fig. 6. It turns out that the solution computed on the meshes which are generated with the help of $\eta_{T,\text{eng}}$ is better.

The efficiency of the global error estimator η can be seen in Fig. 7. Thus, despite the missing of regularity of the solution, the local and global a posteriori error estimators could be applied successfully.

Remark 12. The solutions on the meshes generated by the local a posteriori error estimator $\eta_{T,\text{eng}}$ for the discrete energy norm have been better than on the meshes produced by η_T in Example 11.

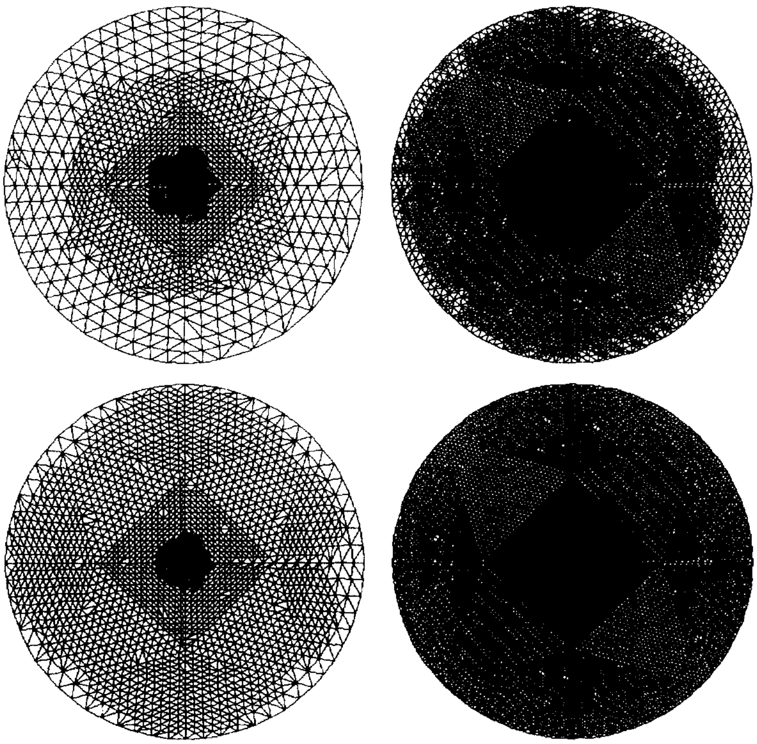

Fig. 6. Example 11, locally refined grids with $\eta_{T,\mathrm{eng}}$ (above) and η_T (below), step 9 and 14.

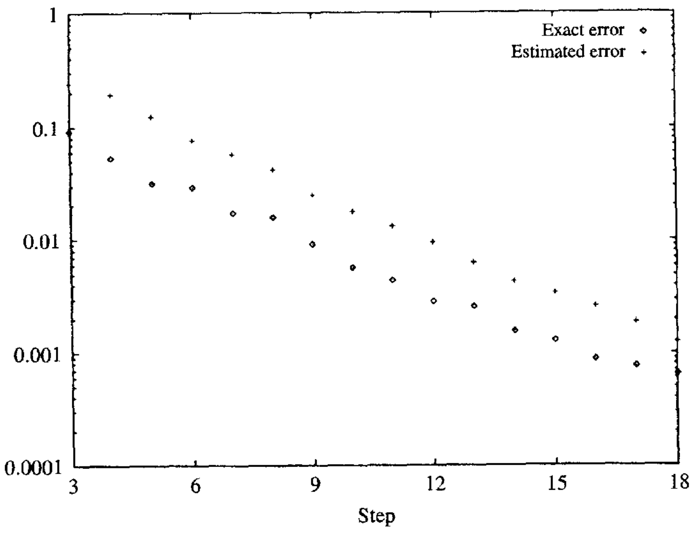

Fig. 7. Example 11, exact and estimated error, adaptive mesh refinement with η_T.

Table 1
Example 11 with uniform refinement, $\eta_{T,\text{eng}}$, and η_T (from top to bottom)

Step	dof velocity	dof pressure	$\|\|u - u_h\|\|_0$	$p_{h,\min}$	$p_{h,\max}$
6	197,376	65,536	1.197-2	−69.6	69.6
7	787,968	262,144	6.017-3	−98.9	98.9
9	12,420	4179	5.719-3	−198.0	198.2
14	83,656	27,979	7.036-4	−1121.3	1121.6
18	352,654	117,749	1.649-4	−4492.9	4457.2
9	12,790	4301	9.038-3	−98.0	98.1
14	67,542	22,639	1.568-3	−276.8	278.2
18	237,298	79,311	6.458-4	−396.2	396.0

We have observed the same for solutions of convection–diffusion equations with one singularity [11]. However, for convection–diffusion equations whose solutions have singularities of different kind we found the meshes of the error estimator in the weaker norm superior.

Remark 13. In a comprehensive study [11], we have applied residual-based a posteriori error estimators for conforming discretizations for the adaptive grid refinement in examples where we have used a nonconforming discretization. The difference of the conforming error estimators to η_T and $\eta_{T,\text{eng}}$ is the missing of the jumps of the discrete function. We have not found any example where the addition of these jump terms has led to clearly different meshes or improved discrete solutions.

Acknowledgements

The author wishes to acknowledge Prof. L. Tobiska for the discussions on the subject of this paper.

References

[1] M. Ainsworth, J.T. Oden, A unified approach to a posteriori error estimation using element residual methods, Numer. Math. 65 (1993) 23–50.
[2] I. Babuška, W.C. Rheinboldt, Error estimates for adaptive finite element computation, SIAM J. Numer. Anal. 15(4) (1978) 283–301.
[3] R.E. Bank, B.D. Welfert, A posteriori error estimates for the Stokes problem, SIAM J. Numer. Anal. 28(3) (1991) 591–623.
[4] P.G. Ciarlet, Basic error estimates for elliptic problems, in: P.G. Ciarlet, J.L. Lions (Eds.), Handbook of Numerical Analysis II, North-Holland, Amsterdam, 1991, pp. 19–351.
[5] Ph. Clément, Approximation by finite element functions using local regularization, RAIRO Anal. Numer. 2 (1975) 77–84.
[6] M. Crouzeix, P.-A. Raviart, Conforming and nonconforming finite element methods for solving the stationary Stokes equations I, RAIRO Anal. Numér. 7 (1973) 33–76.

[7] E. Dari, R. Durán, C. Padra, Error estimators for nonconforming finite element approximations of the Stokes problem, Math. Comp. 64(211) (1995) 1017–1033.

[8] E. Dari, R. Duran, C. Padra, V. Vampa, A posteriori error estimators for nonconforming finite element methods, M2AN 30(4) (1996) 385–400.

[9] O. Dorok, V. John, U. Risch, F. Schieweck, L. Tobiska, Parallel finite element methods for the incompressible Navier–Stokes equations, in: E.H. Hirschel (Ed.), Flow Simulation with High-Performance Computers II, vol. 52 of Notes on Numerical Fluid Mechanics, Vieweg, Braunschweig, 1996, pp. 20–33.

[10] K. Eriksson, D. Estep, P. Hansbo, C. Johnson, Introduction to adaptive methods for differential equations, Acta Numer. (1995) 4, 105–158.

[11] V. John, Parallele Lösung der inkompressiblen Navier–Stokes Gleichungen auf adaptiv verfeinerten Gittern, Ph.D. Thesis, Otto-von-Guericke-Universität Magdeburg, Fakultät für Mathematik, 1997.

[12] V. John, J.M. Maubach, L. Tobiska, Nonconforming streamline-diffusion-finite-element-methods for convection–diffusion problems, Numer. Math. 78 (1997) 165–188.

[13] R. Rannacher, St. Turek, Simple nonconforming quadrilateral stokes element, Numer. Methods Partial Differential Equations 8 (1992) 97–111.

[14] F. Schieweck, A parallel multigrid algorithm for solving the Navier–Stokes equations, Impact Comput. Sci. Engrg. 5 (1993) 345–378.

[15] R. Verfürth, A posteriori error estimates for nonlinear problems, L^r-estimates for finite element discretizations of elliptic equations, Bericht Nr. 199, Ruhr-Universität Bochum, Fakultät für Mathematik, 1996.

[16] R. Verfürth, A Review of A Posteriori Error Estimation and Adaptive Mesh-Refinement Techniques, Wiley and Teubner, New York and Stuttgart, 1996.

[17] R. Verfürth, Robust a posteriori error estimators for the singularly perturbed helmholtz equation, Bericht Nr. 201, Fakultät für Mathematik der Ruhr-Universität Bochum, 1996.

[18] R. Verfürth, A posteriori error estimators for convection–diffusion equations, Bericht Nr. 215, Fakultät für Mathematik der Ruhr-Universität Bochum, 1997.

[19] B. Wohlmuth, Adaptive multilevel-finite-elemente methoden zur lösung elliptischer randwertprobleme, Ph.D. Thesis, Technische Universität München, 1995.